Compensation for Merchant's Circle Diagram to predict cutting force in orthogonal micro turning

WCMNM 2021

Arnab Das[1], Shri Narayan Agnihotri[1], Vivek Bajpai[1]

[1] *Department of Mechanical Engineering, Indian Institute of Technology (ISM) Dhanbad, Jharkhand, India*

Abstract

Cutting force for conventional orthogonal machining can be predicted by Merchant's Circle Diagram (MCD) considering the shearing action of chip formation. However, the effect of ploughing action is significant as well for micro turning which has not been considered in MCD. Therefore, large error has been observed for prediction of cutting force in micro turning by MCD theory. In this study, a compensated model has been developed for orthogonal micro turning based on MCD. The theory has taken shearing and ploughing action into consideration. The compensated model involved material flow stress, cutting parameters and tool geometry including cutting edge radius. This model has predicted tangential cutting force with average prediction error of 3.75% for micro turning of Ti6Al4V. Whereas, the average prediction error was 14.9% for axial cutting force.

Keywords: Merchant's Circle Diagram, Orthogonal micro turning, Cutting force, Cutting edge radius

1. Introduction

Micro turning is a mechanical micromachining technology widely used for fabricating micro valves, micro nozzles, micro moulds in several industries [1]. The stiffness of the micro component is very low so that they may subject to permanent deformation under the action of cutting force. Therefore, the cutting force is required continuous monitoring during micro turning. However, the cutting force monitoring technology is much difficult and expensive process for micro turning. Therefore, the researchers have focused on analytically prediction of cutting force. In general, Merchant's Circle Diagram (MCD) has been used for prediction of cutting force in conventional orthogonal machining. In MCD, the chip formation is assumed by the shearing action [2]. However, the ploughing action has taken a major role in chip formation for micro turning which has not been considered in Merchant's theory. The cutting edge radius is equivalent with the uncut chip thickness resulting in ploughing of the cutting tool on the work surface [3]. This phenomenon significantly increases the cutting force in micro turning. Therefore, the cutting force for micro turning cannot be successfully predicted by MCD theory.

In this study, a compensated model of Merchant's theory has been developed to predict the cutting force for orthogonal micro turning. The model has considered the shearing effect as well as the ploughing effect for chip formation. The material flow stress, cutting parameters and tool geometry including cutting edge radius have been incorporated in the compensated model. Additionally, the model has been validated with some published experimental data for Ti6Al4V. The flow stress of Ti6Al4V has been calculated by modified Johnson-Cook model. The compensated model precipitated 3.75% error in tangential cutting force and 14.9% error in axial cutting force. This model can be applicable for monitoring cutting force in orthogonal micro turning.

2. Modelling of cutting force for orthogonal turning

In general, the cutting force model for orthogonal turning has been established using Merchant's circle diagram. The MCD can be applicable for orthogonal machining only. The geometrical representation of MCD is depicted in Fig. 1.

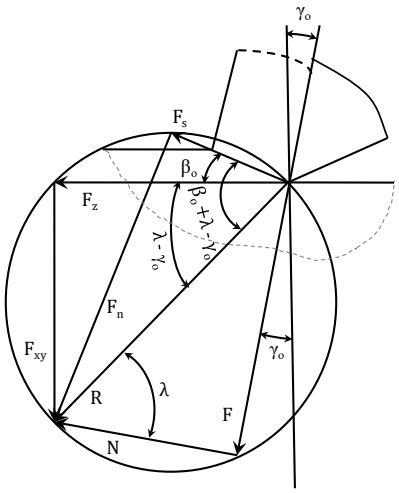

Fig. 1 Merchant's Circle Diagram for cutting force calculation [2]

Based on the diagram, the components of cutting force can be represented as,

$$F_z = \frac{\tau t f \cos(\lambda - \gamma_o)}{\sin\beta_o \cos(\beta_o + \lambda - \gamma_o)} \quad (1)$$

$$F_{xy} = \frac{\tau t f \sin(\lambda - \gamma_o)}{\sin\beta_o \cos(\beta_o + \lambda - \gamma_o)} \quad (2)$$

The axial and radial components of cutting force can be calculated from the following equations,

$$F_x = F_{xy} \sin\emptyset \quad (3)$$

$$F_y = F_{xy} \cos\emptyset \quad (4)$$

From Merchant's theory, the relationship between shear angle, friction angle and orthogonal rake angle has been determined as,

$$2\beta_o + \lambda - \gamma_o = \frac{\pi}{2} \quad (5)$$

The orthogonal rake angle can be estimated from Equation 6,

$$\tan\gamma_o = \tan\gamma_x \sin\emptyset + \tan\gamma_y \cos\emptyset \quad (6)$$

The Merchant's circle diagram is established on single shear plane theory. The shear stress of the work material (τ) can be estimated from the flow stress of the material based on von-mises theory ($\tau = \frac{\sigma}{\sqrt{3}}$) [4]. The flow stress during conventional material removal process (macro level) can be evaluated by Johnson-Cook model [5]. The model depends on cutting strain, strain rate and cutting temperature. The equation to evaluate the flow stress by Johnson-Cook model is depicted in Equation 7.

$$\sigma = [A + B\epsilon^n]\left[1 + C\ln\frac{\dot{\epsilon}}{\dot{\epsilon_o}}\right]\left[1 - \left(\frac{T - T_o}{T_m - T_o}\right)^m\right] \quad (7)$$

Shaw [6] predicted the shear strain of the work material during machining as,

$$\epsilon = \frac{\cot\beta_o + \tan(\beta_o - \gamma_o)}{\cos\eta_s} \quad (8)$$

The shear flow angle (η_s) is related to chip flow angle (η_c) as Equation 9. For orthogonal machining, the chip flow angle is same as the chip flow deviation angle (ψ) due to restricted cutting edge effect ($\eta_c = \psi$). Additionally, the chip flow deviation angle can be evaluated from Equation 10 [7].

$$\tan\eta_s = \frac{-\tan\eta_c \sin\beta_o}{\cos\gamma_o} \quad (9)$$

$$\tan\psi = \frac{\sin(\emptyset_{avg} + \emptyset_1)}{\cos(\emptyset_{avg} + \emptyset_1) + \frac{2t}{a_o \sin\emptyset_{avg}}} \quad (10)$$

$$\emptyset_{avg} = \frac{\frac{\emptyset}{2} + \left[\frac{t}{r} + \cos\emptyset - 1\right]\frac{1}{\sin\emptyset}}{1 + \frac{\left[\frac{t}{r} + \cos\emptyset - 1\right]}{\emptyset\sin\emptyset}} \quad (11)$$

Shaw [6] proposed a model to predict the shear strain rate in machining process based on shear velocity and adiabatic shear band spacing.

$$\dot{\epsilon} = \epsilon\frac{V_s}{\Delta y} \quad (12)$$

Where, the shear velocity (V_s) can be calculated as,

$$V_s = V_c\frac{\cos\gamma_o}{\cos(\beta_o - \gamma_o)} \quad (13)$$

The mathematical model of adiabatic shear band spacing has been established by Huang and Aifantis [8] and expressed as Equation 14.

$$\Delta y = £\left(\frac{m\, a_o \sin\beta_o}{\cos\gamma_o}\right) \quad (14)$$

£ is termed as Taylor-Quinney coefficient. This estimates the fraction of plastic energy transformed into heat while the material removal process. It is usually considered as 0.9 [7].

3. Calculation of cutting force for macro turning

The cutting forces have been calculated for orthogonal macro turning. A research paper has been selected for turning of Ti6Al4V. The flow shear stress of Ti6Al4V has been calculated from the Johnson-Cook model. Lee and Lin [9] model has been used to select the Johnson-Cook materials constant for Ti6Al4V. The materials constants have been enlisted in Table 1. The temperature of the workpiece in the machining zone (T) has been considered from the experimental value of previous literatures. This has been incorporated in the Johnson-Cook model. In general, the material shows null deformation upto the value of its yield stress and the strain increases rapidly with low to moderate strain gradient beyond the yield stress [10]. Hence, Ti6Al4V can be considered as a rigid perfectly plastic material and fulfils the initial assumption of Merchant's theory.

Table 1 Johnson-Cook material model for Ti6Al4V [9]

A (MPa)	B (MPa)	C	m	n	T_o (ºC)	T_m (ºC)
782.7	498.4	0.028	1	0.28	20	1660

The process parameters has been selected for the calculation of cutting force according to the experiments performed by Boujelbene [11]. The process parameters and the tool geometry used for the modelling have been depicted in Table 2. The friction angle and shear angle have been estimated as 19.21º and 32.4º respectively.

Table 2 Machining parameters for calculation of cutting force

Orthogonal rake angle	−6º
Principal cutting edge angle	90º
Nose radius (mm)	0.8
Cutting speed (m/min)	50
Feed rate (mm/rev)	0.1 and 0.2
Depth of cut (mm)	1

Based on the machining parameters, the main cutting force component (F_z) has been predicted using MCD model. The calculated cutting forces have shown good similarities with experimental results as found by Boujelbene [11]. The comparisons of calculated and experimental cutting forces have been depicted in Fig. 2. The errors for both the cases were within 5% as shown in the Fig. 2.

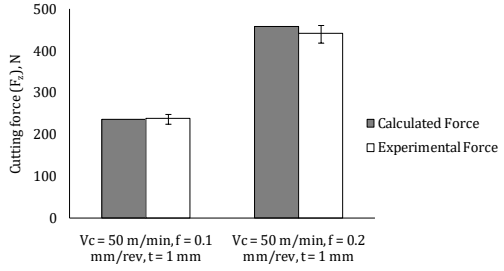

Fig. 2 Comparison of cutting forces calculated with MCD and determined in experiments

4. Modelling and compensation of Merchant's

Circle Diagram for micro turning

Micro turning is much different from conventional macro turning due to its small scaling issues. The invariance of uncut chip thickness and the cutting edge radius has resulted in some ploughing effect in micro turning. The ploughing effect has not been considered in Merchant's Circle Diagram. Additionally, deformation of low thickness due to small depth of cut resulted in significant increase of flow stress in work material. These need to be compensated for Merchant's Circle Diagram. The flow chart of modified cutting force model for orthogonal micro turning has been depicted in Fig. 3.

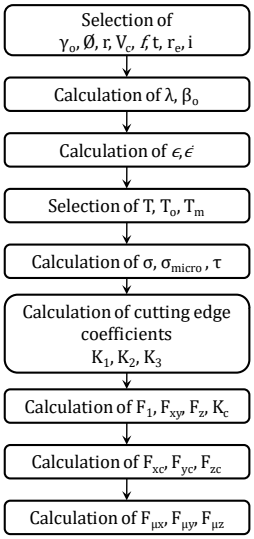

Fig. 3 Flowchart of modified cutting force model for orthogonal micro turning

For scaling issues of micro turning, strain gradient is significant for lower strain and cutting speed. Therefore, the effect of strain gradient has been incorporated in Johnson-Cook model by Jagadesh and Samuel [7]. The modified version of Johnson-Cook model has been proposed by Lai et al. [12] compensating the strain gradient effect and represented in Equation 15. In this Equation, G = 44 GPa as per standard value, Magnitude of burger vector b = 0.295 nm, Geometrical dislocation density χ = 0.38 and a is an empirical constant (a = 0.25). Additionally, the mathematical expression of effective strain gradient (η) has been developed by Tounsi et al. [13] and expressed in Equation 16. Rao and Shunmugam [14] investigated the thickness of plastic shear zone (h) as half of the uncut chip thickness.

$$\sigma_{micro} = \sigma \sqrt{1 + \left(\frac{18a^2bG^2\eta}{\sigma^2}\right)^{\chi}} \tag{15}$$

$$\eta = \frac{2\cos\gamma_o}{\sqrt{3}h\cos(\beta_o - \gamma_o)\sin\beta_o} \tag{16}$$

The uncut chip thickness in micro turning is equivalent with the cutting edge radius as depicted in Fig. 4. As a result, the effective rake angle becomes negative for micro turning process leading to significant ploughing effect on the work surface [3]. This phenomenon significantly increases the specific cutting energy as well as cutting force.

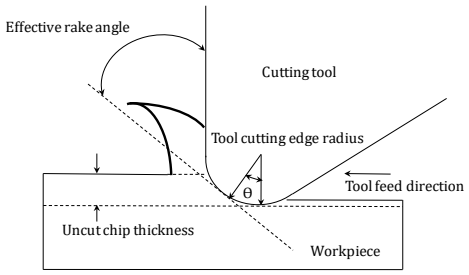

Fig. 4 Effect of tool cutting edge radius in micro turning

Abdelmoneim and Scrutton [15] developed an analytical model to compensate the influence of cutting edge radius based on stagnation angle and shear stress of the work material. The cutting edge coefficients can be represented as,

$$K_{te} = r_e\tau\left(\frac{2\theta}{\cos\theta} + \pi\sin\theta\tan\theta\right) \tag{17}$$

$$K_{re} = r_e\tau\left(2\sqrt{3}\sin\theta\right) \tag{18}$$

$$K_{ae} = K_{te}\sin i \tag{19}$$

The value of stagnation angle has been considered as 14° for micro cutting processes [14]. Therefore, the cutting edge coefficients can be modified incorporating the width of cut $\left(w_o = \frac{t}{\sin\beta_o}\right)$ as,

$$K_1 = \frac{0.693\, r_e\tau t}{\sin\beta_o} \tag{20}$$

$$K_2 = \frac{0.838\, r_e\tau t}{\sin\beta_o} \tag{21}$$

$$K_3 = K_1\sin i \tag{22}$$

The mechanistic model of cutting force developed by Jagadesh and Samuel [7] was based on the cutting coefficients for oblique cutting. The model can be modified for orthogonal turning operation. The frictional force component due to chip flow deviation by restricted cutting edge and nose radius along the flank face can be expressed as,

$$F_1 = \frac{\tau t f \sin\lambda\,(-\tan\eta_c)\cos i}{\sin\beta_o\cos(\beta_o + \lambda - \gamma_o)} \tag{23}$$

Based on the theory, the cutting force elements due to tool geometry (without considering cutting edge effect) can be expressed as,

$$\begin{bmatrix} F_{xc} \\ F_{yc} \\ F_{zc} \end{bmatrix} = K_c \begin{bmatrix} F_{xy} & 0 & F_{xy} \\ \cos\gamma_o\, F_1 & -\sin\gamma_o\, F_z & F_{xy} \\ \sin\gamma_o\, F_1 & \cos\gamma_o\, F_z & F_{xy} \end{bmatrix} \begin{bmatrix} \int_{\emptyset}^{0} \sin\emptyset\, d\emptyset \\ \int_{\emptyset}^{0} \sin\emptyset\, d\emptyset \\ \int_{\emptyset_1}^{0} \sin\emptyset_1\, d\emptyset_1 \end{bmatrix} \tag{24}$$

In this equation, K_c is constant and can be expressed as,

$$K_c = \frac{1}{\sin\beta_o\cos i} \tag{25}$$

F_z and F_{xy} are the cutting force components calculated from Merchant's Circle Diagram. Therefore, the total cutting force components for

orthogonal micro turning can be expressed as,

$$\begin{bmatrix} F_{\mu x} \\ F_{\mu y} \\ F_{\mu z} \end{bmatrix} = \begin{bmatrix} F_{xc} \\ F_{yc} \\ F_{zc} \end{bmatrix} + \begin{bmatrix} K_3 & 0 & K_3 \\ \cos\gamma_o K_1 & -\sin\gamma_o K_2 & K_3 \\ \sin\gamma_o K_1 & \cos\gamma_o K_2 & K_3 \end{bmatrix} \begin{bmatrix} \int_{\emptyset}^{0} d\emptyset \\ \int_{\emptyset}^{0} d\emptyset \\ \int_{\emptyset_1}^{0} d\emptyset_1 \end{bmatrix} \quad (26)$$

The micromachining force with depth of cut in the micron range (1 µm – 100 µm) can be predicted by this model. However, the machining in the submicron range (Depth of cut below 1 µm) has not been considered in this model.

5. Validation of the model

For validation of the compensated model, experimental results has been taken from a published research paper by Jagadesh and Samuel [7]. The micro turning operation has been performed on Ti6Al4V. The shear stress of Ti6Al4V has been determined applying Johnson-Cook model using the Johnson-Cook constants as mentioned in Table 1. The tool geometry has been enlisted in Table 3 which has been used for calculation. Table 4 depicts the machining conditions which have been used for the model.

Table 3 Tool geometry for the experiments [7]

Orthogonal rake angle	6º
Principal cutting edge angle	95º
Auxiliary cutting edge angle	15º
Nose radius (mm)	0.8
Included angle	80º
Cutting edge radius (µm)	15

Table 4 Machining conditions

Experiment No.	Cutting speed (m/min)	Feed rate (µm/rev)	Depth of cut (µm)
Experiment 1	19	20	30
Experiment 2	19	20	10
Experiment 3	19	20	20
Experiment 4	19	15	30
Experiment 5	19	25	30

For the first experiment, the friction angle and shear angle have been calculated as 19.21º and 38.4º. The strain and strain rate was 1.896 and 0.64×10^5/s. T, T_o, T_m have been selected as 500ºC, 20ºC, 1660ºC respectively. From these values; σ, σ_{micro} and τ have been estimated as 963 MPa, 1302 MPa and 751.76 MPa respectively. Further, K_1, K_2, K_3 have been calculated as 0.377, 0.456 and 0.371 respectively. F_1, F_{xy}, F_z, K_c have been estimated as 1.73×10^{-5} N, 0.267 N, 1.138 N and 9.27 respectively. Eventually, $F_{\mu x}$ and $F_{\mu z}$ have been determined as 3.485 N and 12.40 N respectively. Fig. 5 represents the comparisons of calculated and experimental cutting forces along tangential and axial directions. The comparisons show good similarities between both the results. The average prediction error is 3.75% for the tangential cutting force components (main cutting force). However, the prediction error is 14.9% for axial cutting force components (feed force). It has been observed that the prediction error is higher for lower values of the axial force components. However, the prediction errors do not vary significantly for lower or higher values of tangential cutting forces. Hence the compensated model can successfully predict the cutting force for orthogonal micro turning operation. In general, the Merchant's theory predicted the deformation across a thin shear plane. However, the strain gradient became significant due to small uncut chip thickness during micro turning; and the flow stress and shear stress of the work material have been modified. Sometimes, the shear stress has been overestimated as compared to the actual shear stress developed. Due to this phenomenon, the calculated cutting force has been exceeded the experimental one in some cases.

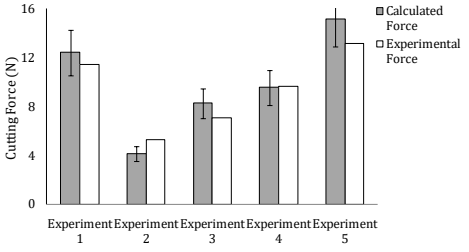

(a) Tangential cutting force components ($F_{\mu z}$)

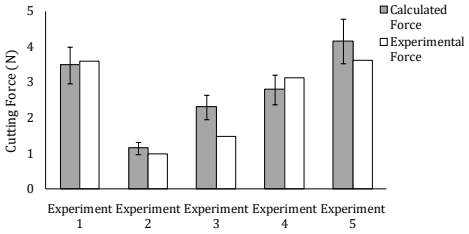

(b) Axial cutting force components ($F_{\mu x}$)

Fig. 5 Comparison of calculated and experimental cutting force

6. Conclusions

The Merchant's Circle Diagram can predict the cutting forces for orthogonal machining based on shear plane theory. However, for micro turning operation, the chip formation mechanism is based on shearing and ploughing action which has not been considered in Merchant's Circle Diagram. Therefore, it cannot predict the cutting force for micro turning accurately. In this paper, a compensated model of Merchant's Circle Theory has been developed for orthogonal micro turning operation. The model has taken the cutting parameters, tool geometry including the cutting edge radius into consideration. The compensated model can successfully predict the cutting force components for orthogonal micro turning. The average prediction error was 14.9% for axial components of cutting force. Whereas, this is 3.75% for tangential component of cutting force.

Nomenclature

F_z	Main (Tangential) cutting force calculated from MCD, N
F_{xy}	Normal component of main cutting force calculated from MCD, N
F_s	Shear force calculated from MCD, N
F_n	Force acting normal to the shear plane calculated from MCD, N
F	Frictional force on the chip-tool interface calculated from MCD, N

N	Normal force on the chip-tool interface calculated from MCD, N
R	Resultant force calculated from MCD, N
F_x	Axial cutting force component calculated from MCD, N
F_y	Radial cutting force component calculated from MCD, N
λ	Friction angle, rad
γ_o	Orthogonal rake angle, rad
β_o	Shear angle, rad
τ	Shear stress of the work material, MPa
t	Depth of cut, μm or mm
f	Feed rate, μm/rev or mm/rev
$\emptyset$	Principal cutting edge angle, rad
γ_x	Side rake angle, rad
γ_y	Back rake angle, rad
σ	Flow stress of the work material, MPa
A	Yield strength of work material, MPa
B	Strain hardening modulus, MPa
C	Strain rate sensitivity coefficient
m	Thermal softening coefficient
n	Hardening coefficient
ϵ	Plastic strain
$\dot{\epsilon}$	Strain rate, s^{-1}
$\dot{\epsilon_o}$	Reference strain rate, s^{-1}
T	Workpiece temperature, ^oC
T_o	Ambient temperature, ^oC
T_m	Melting temperature of workpiece, ^oC
η_s	Shear flow angle, rad
η_c	Chip flow angle, rad
ψ	Chip flow deviation angle due to restricted cutting edge effect, rad
$\emptyset_1$	Auxiliary cutting edge angle, rad
a_o	Uncut chip thickness, μm
r	Tool nose radius, μm
V_c	Cutting speed, m/min
V_s	Shear velocity, m/min
Δy	Adiabatic shear band spacing, mm
σ_{micro}	Flow stress of work material during micro turning, MPa
a	Empirical constant
b	Magnitude of burger vector, nm
G	Shear modulus, MPa
η	Effective strain gradient, μm^{-1}
χ	Geometric dislocation density
r_e	Cutting edge radius, μm
Θ	Stagnation angle
K_{te}	Tangential cutting edge coefficient
K_{re}	Radial cutting edge coefficient
K_{ae}	Axial cutting edge coefficient
£	Taylor-Quinney coefficient
h	Plastic shear zone thickness, μm
w_o	Width of cut, μm
i	Included angle, rad
F_{xc}	Axial cutting force component without considering cutting edge effect, N
F_{yc}	Radial cutting force component without considering cutting edge effect, N
F_{zc}	Tangential cutting force component without considering cutting edge effect, N
$F_{\mu x}$	Axial cutting force for micro turning, N
$F_{\mu y}$	Radial cutting force for micro turning, N
$F_{\mu z}$	Tangential (main) cutting force for micro turning, N

References

[1] S. Singh et al., "Effect of machining parameters on cutting force during micro-turning of a brass rod," Mater. Manuf. Process., 2019; 6914.

[2] M. E. Merchant, "Mechanics of the metal cutting process. I. Orthogonal cutting and a type 2 chip," J. Appl. Phys., 1945.

[3] X. Wu et al., "Experimental investigation of specific cutting energy and surface quality based on negative effective rake angle in micro turning," Int. J. Adv. Manuf. Technol., 2016.

[4] W. D. Nix et al., "Indentation size effects in crystalline materials: A law for strain gradient plasticity," J. Mech. Phys. Solids, 1998.

[5] G. R. Johnson et al., "Fracture characteristics of three metals subjected to various strains, strain rates, temperatures and pressures," Eng. Fract. Mech., 1985.

[6] M. C. Shaw, Metal cutting principles: Chapter 3: 2005.

[7] T. Jagadesh et al., "Mechanistic and Finite Element Model for Prediction of Cutting Forces during Micro-Turning of Titanium Alloy," Mach. Sci. Technol., 2015.

[8] J. Huang et al., "Note on the problem of shear localization during chip formation in orthogonal machining," J. Mater. Eng. Perform., 1997.

[9] W. S. Lee et al., "High-temperature deformation behaviour of Ti6A14V alloy evaluated by high strain-rate compression tests," J. Mater. Process. Technol., 1998; 75(1–3): 127–136.

[10] J. Sun et al., "Material flow stress and failure in multiscale machining titanium alloy Ti-6Al-4V," Int. J. Adv. Manuf. Technol., 2009.

[11] M. Boujelbene, "Investigation and modeling of the tangential cutting force of the Titanium alloy Ti-6Al-4V in the orthogonal turning process," in Procedia Manufacturing, 2018.

[12] X. Lai et al., "Modelling and analysis of micro scale milling considering size effect, micro cutter edge radius and minimum chip thickness," Int. J. Mach. Tools Manuf., 2008.

[13] N. Tounsi et al., "From the basic mechanics of orthogonal metal cutting toward the identification of the constitutive equation," Int. J. Mach. Tools Manuf., 2002.

[14] S. Rao et al., "Analytical modeling of micro end-milling forces with edge radius and material strengthening effects," Mach. Sci. Technol., 2012.

[15] M. E. Abdelmoneim et al., "Tool edge roundness and stable build-up formation in finish machining," J. Manuf. Sci. Eng. Trans. ASME, 1974.